Biuletyn WAT
Vol. LXVII, Nr 4, 2018

Estimate of dynamic load capacity of reinforced concrete deep beam made of very high strength construction materials

WALDEMAR CICHORSKI

Military University of Technology, Faculty of Civil Engineering and Geodesy,
Department of General Construction, 2 Gen. W. Urbanowicza Str., 00-908 Warsaw, Poland,
waldemar.cichorski@wat.edu.pl

Abstract. The paper presents an analysis of the dynamic load capacity of a dynamically loaded rectangular reinforced-concrete deep beam made of high-strength materials, including the physical nonlinearity of the construction materials: concrete and reinforcing steel. The solution was acquired with the use of the method presented in [15]. The dynamic load capacity of the reinforced concrete beam was determined. The results of numerical solutions are presented, with particular emphasis on the impact of the very high strength of concrete and steel on the reinforced concrete beam's dynamic load capacity. The work confirmed the correctness of the assumptions and deformation models of concrete and steel as well as the effectiveness of the methods of analysis proposed in the paper [1, 15] for the problems of numerical simulation of the behaviour of reinforced concrete deep beams under dynamic loads.
Keywords: mechanics of structures, reinforced concrete structures, deep beams, dynamic load, physical nonlinearity
DOI: 10.5604/01.3001.0012.8483

1. Introduction

The aim of the work is the analysis of the impact of the very high strength of concrete and reinforcement steel on the load capacity of rectangular reinforced concrete deep beams loaded dynamically with the inclusion of physical nonlinearity of the construction materials: concrete and steel. The solution was acquired with the use of the method of analysis of non-elastic behaviour of reinforced dynamically loaded concrete deep beam in [15].

The essence of this method consists of the following elements: dynamic modelling of the material properties, modelling of the process of deformation of the flat construction framework — reinforced concrete deep beam, and also algorithmisation and numeric programming of the solution. Modelling of the properties of construction materials was carried out with the use of the assumptions of the flow plasticity theory. The model of plastic/ideally viscoplastic material was used for the reinforcement steel, taking into account the plastic retardation effect. Modelling the dynamic properties of concrete has been a topic of the consideration of many publications, i.e. [9, 18]. Constitutive modelling of high-value and ultra-high-grade concrete properties was the subject of study in [8]. For concrete, a non-standard model of dynamic deformation was adopted in [4, 14]. This model describes the elastic properties of concrete, the limited properties of ideal viscoplasticity on the initial dynamic surface of plasticity, material weakening and volume changes. The degradation of the deformation module was ignored in the model. The adopted concrete model facilitates a simplified description of material scratching or crushing as states of loss of load capacity achieved in the process of material weakening. A reduced form of the dynamic concrete model [14] was adopted in the study, reduced to the state of flat stress, both for loading and unloading processes. The limit curve for the adopted concrete model is shown in Fig. 1.

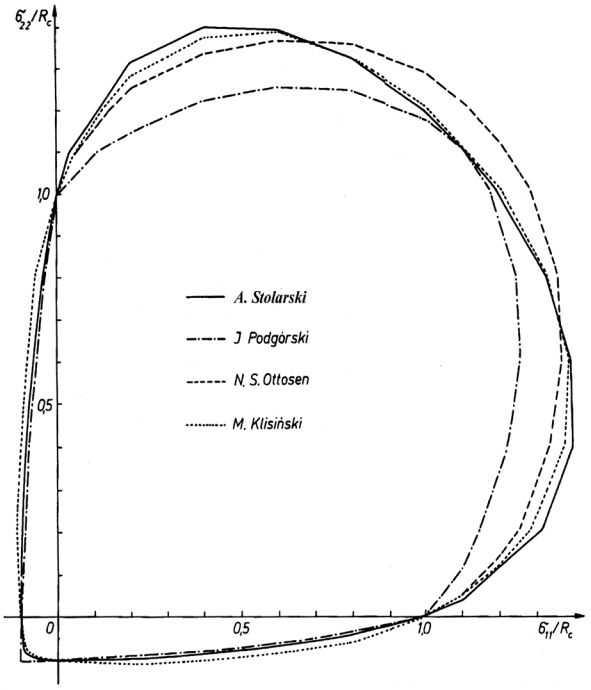

Fig. 1. Limit curve for the adopted concrete model [14] in a flat stress state

Achieving the goal required the introduction of constant properties into the adopted concrete model, allowing the description of the properties of a concrete of very high strength. An assumption was adopted, in the modified concrete model, that the boundary deformation values may be variable and dependent on the class of concrete [1, 16]. The analysis method of the effort of the construction form was formulated with the use of the principles of the finite element method [5]. For the reinforced concrete deep beam, treated as a composite material consisting of a concrete matrix strengthened with thin rods of steel reinforcing, a hypothesis for the cooperation of the reinforcing rods and matrix material was proposed. The solution of dynamic systems of the displacement equations for the displacement of the finite element method was conducted based on algorithms and programmes of numerical analysis of the flat tension state, which allows the identification of the states of displacement, deformation, and deformation and tension speed with the inclusion of the effects of physical material nonlinearity, including concrete scratching.

In this study, the results are presented of numerical solutions for a reinforced concrete deep beam, which was the topic of static experimental research of F. Loenhardt and R. Walter, [6]. As part of the study, the load capacity of a reinforced concrete deep beam was determined in the dynamic deformation process. The impact of the very high concrete and reinforcing steel strength on the dynamic load capacity of reinforced concrete beams was analysed, taking into account the physical non--linearities of the construction materials.

2. Subject of the analysis

The subject of the analysis are deep beams made of a concrete matrix strengthened with thin, steel reinforcement rods in an orthogonal arrangement. The deep beam is loaded on the upper edge with a constant-over-time and equally distributed dynamic load $p(x,t) = p = \text{const}$.

Analysis of damage to various types and sizes of beams made of high-grade concretes was discussed in [4, 11, 12].

A numerical analysis was applied to a rectangular reinforced concrete deep beam with orthogonally arranged reinforcement, designated in the paper of F. Leonhardt and R. Walther [6] as WT3 (Fig. 2). The deep beam was the subject of the analysis in the paper [2, 7].

The dimensions of the deep beam are: length, breadth: $L = B = 160$ cm, thickness: $t = 10$ cm. The main reinforcement of the deep beam was made in the form of 4 layers of reinforcement loops with a yield point of $f_y = 410$ MPa, a diameter of the rods of $\phi 8$, placed in the lower part of the deep beam. The remaining part of the deep beam was reinforced with vertical and horizontal stirrup reinforcement made of steel with a yield point of $f_y = 240$ MPa, a diameter of the rods of $\phi 5$, and

spacing of 26 cm. The concrete matrix was made of concrete with a compression strength of f_c = 30 MPa and an elongation strength of f_t = 3 MPa.

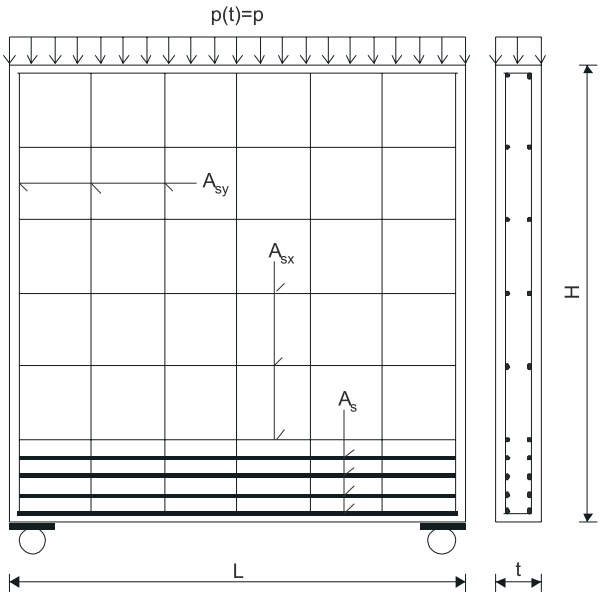

Fig. 2. Reinforced concrete deep beam diagram

Taking into account the use in the numerical construction analysis of high strength concrete, paper [17] included a proposed modification of the concrete deformation model. The essence of the proposed modification of the concrete model is a change in the interpretation of the size of boundary deformation ε_{fc} for the phase of ideal viscoplasticity and ε_{uc} for the phase of material weakening. In the basic version of the model, on the basis of the analysis of the results of experimental research, boundary deformations ε_{fc} are determined as constant values for single--axis compression of 2 ‰, regardless of the concrete class, whereas for boundary deformations ε_{uc}, the values were determined within the range of ε_{uc} = (6 - 12)‰, on the condition that lower values ε_{uc} may be used for concrete of higher class, and higher values ε_{uc} for concrete of lower and medium class, but without an exact designation of the relation with the concrete class. Currently, in the modified concrete deformation model, it is assumed that the boundary deformation values ε_{fc} and ε_{uc} may be variable and dependent on the concrete grade, in accordance with the concrete strength variability function specifying the so-called strength indicator, as described in paper [17].

As a consequence, material properties describing the constitutive concrete model, shown in Table 1, were adopted for the numerical analysis.

Table 1

Boundary parameter values describing the concrete model

Concrete grade	f_c [MPa]	f_t [MPa]	ε_{ec} [‰]	ε_{fc} [‰]	ε_{uc} [‰]	E_c [GPa]
C30	30	3	1.20	2.00	12.00	25.0
C100	100	10	2.08	2.80	11.25	48.0
C200	200	20	3.88	4.49	10.71	51.50
C300	300	30	5.71	6.21	10.21	52.5

A graphic interpretation of the material parameters describing the constitutive concrete model is shown in Fig. 3, in the plane of stresses and deformation for single--axis compression. In this picture, the indicator Ψ_d describes the dynamic strength of concrete in accordance with the model described in the paper [14].

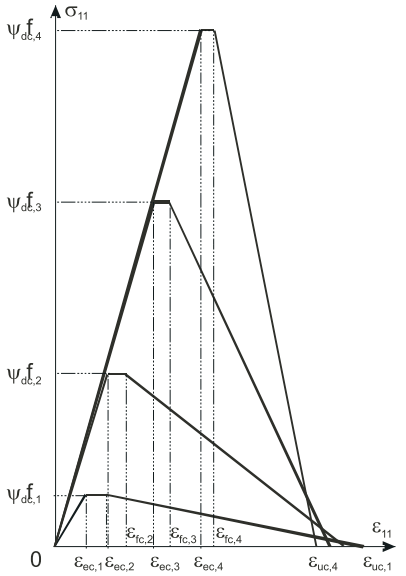

Fig. 3. Graphic interpretation of material parameters of the constitutive concrete model.

For increased strength steel, a modification was made to the steel strength parameters of the main reinforcement of the deep beam, i.e. rods with a diameter of $\phi 8$. The modification involved using steel class $A - H$ with a yield point of $f_y = 690$ MPa.

The intensity of the dynamic load designates the dimensionless parameter $\alpha = P/P_0$ of auxiliary, total load of the deep beam $P_0 = p \times L$, in relation to the level of static deep beam carrying capacity P_0. Assessment of the level of static deep beam carrying capacity in relation to each deep beam type, in accordance with [3], amounts to:

— for C100, C200, C300 concrete and A-III steel: P_0 = [2210 kN/2595 kN/3317 kN]
— for C100, C200, C300 concrete and A-H steel: P_0 = [2085 kN/3028 kN/3999 kN].

The following Figures show diagrams of the vertical displacement of point x_d on the lower edge in the middle cross-section (designation as per Fig. 6) as a function of the static load $P = p \times L$, for regular (Fig. 4) and high-strength (Fig. 5) steel grades.

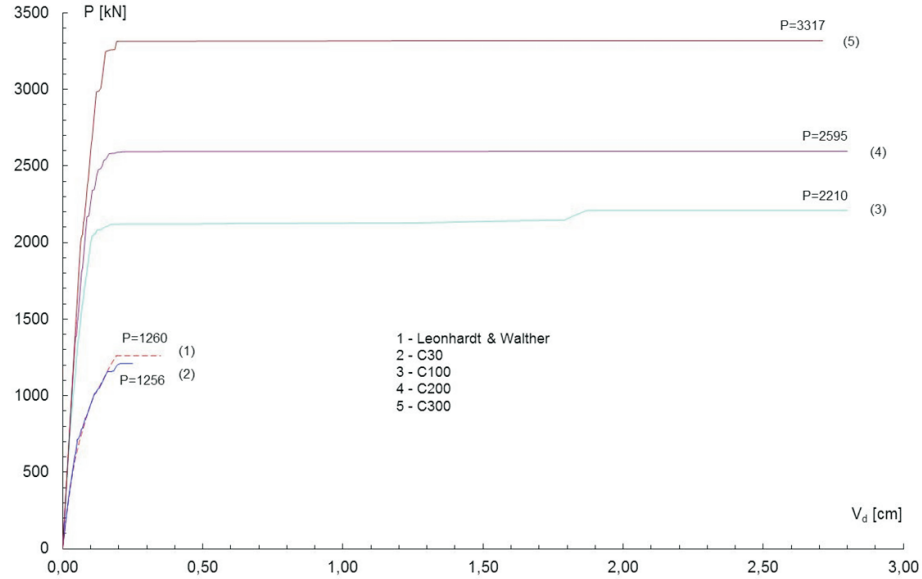

Fig. 4. Load – displacement relation in deep beam's middle lower edge point, reinforcement steel grade A – III

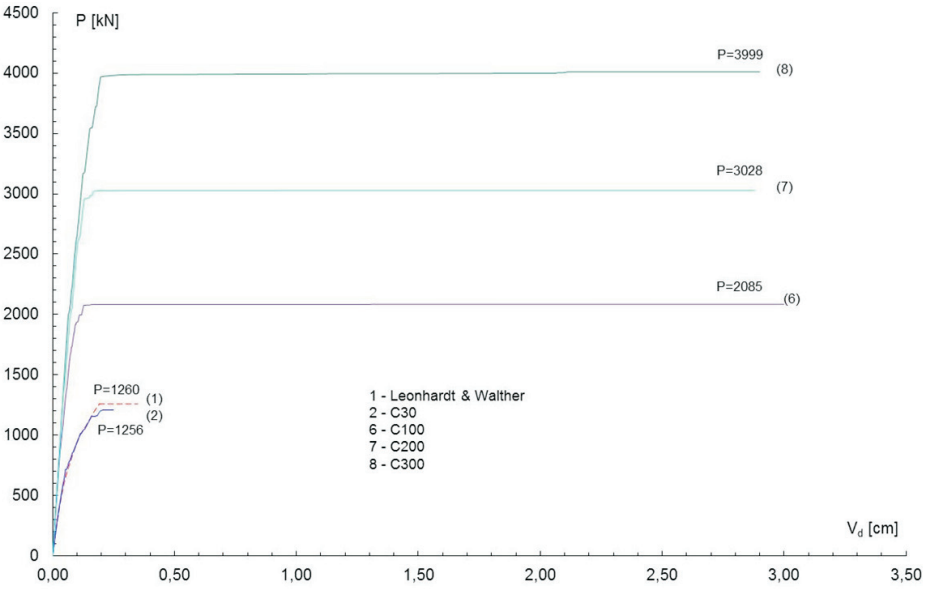

Fig. 5. Load - displacement relation in deep beam's middle lower edge point, reinforcement steel grade A – H

3. Dynamic load capacity of reinforced concrete deep beam

To illustrate the impact of high-strength concrete on the dynamic load capacity of rectangular reinforced concrete deep beams, numerical experiments were carried out for a beam with the reinforcement arranged like in experiment [6] and with modified parameters describing the constitutive model of concrete (concrete grade C100, C200, C300). Additionally, the impact of changing the strength parameters of the reinforcing steel, i.e. the impact of swapping *A-III* ordinary steel, similarly to experiment [6], for *A-H* steel with increased strength, was analysed.

For that purpose, the following points in the central section (designated in Fig. 6) were adopted for the observation of dynamic changes of displacement of the deep beam: x_d – lower edge, x_s – half beam height x_g – upper edge.

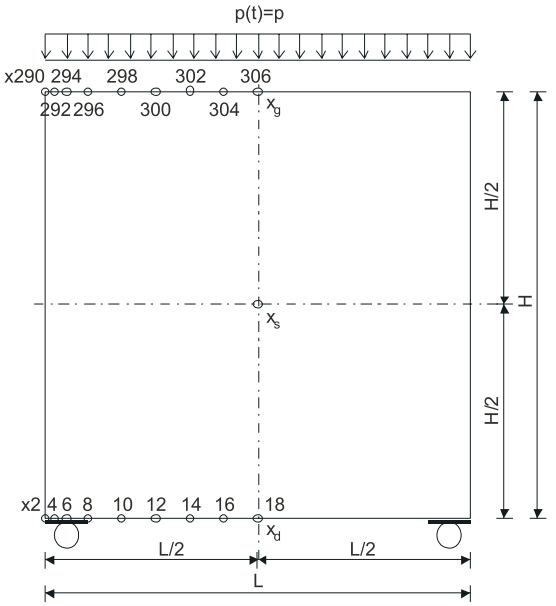

Fig. 6. Designation of points chosen for observation

In turn, the following points were selected for observation in order to illustrate the variability over time of the lower and upper edge of the deep beam:

— on the lower edge of the deep beam: x_2, x_4, x_6, x_8, x_{10}, x_{12}, x_{14}, x_{16}, x_{18},

— on the upper edge of the deep beam: x_{290}, x_{292}, x_{294}, x_{296}, x_{298}, x_{300}, x_{302}, x_{304}, x_{306},

the designations of which were show in Fig. 6.

Based on observations of changes in the beam's dynamic displacement at selected points, its dynamic load capacity was determined. The deep beam's dynamic load capacity is defined as the highest load at which the beam is still vibrating around the equilibrium corresponding to permanent displacements.

Fig. 7 shows, for *C100* concrete and regular *A-III* steel reinforcement, the relation between the permanent dynamic displacements in selected points and the load. Fig. 7_1 shows the variability of the permanent dynamic displacement of selected points in the middle cross-section under various loads $\alpha = P/P_0$. For a load level of $\alpha = 0.3$, in the elastic range and with a minor level of plastic processes in the concrete, the results indicate the relation known from elastic solutions between vertical displacements: $v(x_g) > v(x_s) > v(x_d)$. As the load increases to the level of $\alpha = 0.4$, a significant increase of vertical displacements of the lower point x_d is observed. Because of the cracks (scratching) of the concrete in the lower layers of the shear zone, there was a partial modification of the interrelation of the changes of individual vertical displacements over time: $v(x_g) > v(x_d) > v(x_s)$. Upon further application of load to the level of $\alpha = 0.5$, the propagation of scratched areas occurred in the shear zone (in two directions, upwards and diagonally towards the direction of the centre of the span) and in the span area, which caused another modification of interrelations between the change over time of each vertical displacement: $v(x_s) > v(x_d) > v(x_g)$, which applies at intervals of reaching the maximum amplitude of displacements. At a load level of $\alpha = 0.6$, a lack of plastic process stabilisation can be observed, which ultimately led to the beam's lost load capacity.

Fig. 7_2 shows the variability of the permanent dynamic vertical displacement in selected points in the lower edge of the deep beam under various loads $\alpha = P/P_0$. Within the structure's plastic capacity range, at load levels of $\alpha = 0.1$ and $\alpha = 0.2$, the maximum permanent displacement occurred in the span at point x_{18}, and the observed amplitude values of vertical displacements decreased monotonically towards the support. The same behaviour of the structure was observed at a load level of $\alpha = 0.3$, when cracking of the concrete in proximity of the support occurred. At a load level of $\alpha = 0.4$, a sudden increase in the displacement of point x_{10} can be observed, below the value of displacement of points in proximity of the central axis of the vertical symmetry. It is caused by the development of the area of scratched concrete in the proximity of that point — a propagation of the scratched area occurred in the vertical direction. Upon an additional increase of load to $\alpha = 0.5$, stabilisation of displacement of point x_{10} is observed. At the same time, a sudden increase in permanent vertical displacements can be observed in the following points: x_{12}, x_{14}, x_{16}, x_{18} in relation to the manifestation of a new scratch area in the central section and with the change of propagation of scratched area in the shear zone from vertical to diagonal towards the central section. Under a load of $\alpha = 0.6$, an unimpeded increase in vertical displacements occurred successively in points x_{16}, x_{18}, x_{14} — it is a clear sign of the depletion of the carrying capacity and destruction of the analysed deep beam.

Fig. 7_3 shows variability of the permanent dynamic vertical displacement in the selected points in the upper edge of the deep beam under various loads $\alpha = P/P_0$. The maximum permanent deflection occurred in the span at point x_{306}, and the observed amplitudes of permanent vertical displacements decreased monotonously towards the support.

Fig. 8 shows, for *C200* concrete and regular *A-III* steel reinforcement, the relation between the permanent dynamic displacements in selected points and the load.

Fig. 8_1 shows the variability of the permanent dynamic displacement of selected points in the middle cross-section under various loads $\alpha = P/P_0$. Up to the load level of $\alpha = 0.3$, like in the reinforced *C100* concrete deep beam, the structure reacted in the elastic range at a low level of plastic processes in the concrete; the results indicated an analogical relation between the vertical displacements: $v(x_g) > v(x_s) > v(x_d)$. As the load increases to the level of $\alpha = 0.4$, a significant increase of vertical displacements of the lower point x_d is observed. Because of the cracks (scratching) of the concrete in the lower layers of the shear zone, there was a partial modification of the interrelation of the changes of individual vertical displacements over time: $v(x_g) > v(x_d) > v(x_s)$. As the load was increased to $\alpha = 0.5$, a propagation of the crack areas occurred that was different from the propagation in the *C100* concrete deep beam, i.e. the propagation was observed in the shear zone only (and in two directions: upwards and diagonally towards the span centre). The effect of this was unlike in the *C100* concrete deep beam: it did not modify the interrelation of the changes of individual vertical displacements over time, i.e. $v(x_g) > v(x_d) \cong v(x_s)$. Under a load of $\alpha = 0.6$, as an effect of the development of the concrete crack zones in one area, diagonally from the shear zone to the upper layers of the span cross-section, the carrying capacity of the deep beam was lost.

Fig. 8_2 shows the relation between the permanent vertical displacement in selected points in the deep beam's lower edge and the various loads $\alpha = P/P_0$. In the range of elastic capacity of the structure, the loads $\alpha = 0.1$ and $\alpha = 0.2$ gave the maximum deflection, just like in the *C100* concrete deep beam's span at point x_{18}, and the observed amplitude values of the vertical displacements decreased monotonously towards the support. The same behaviour of the structure was observed at a load level of $\alpha = 0.3$, when the cracking of the concrete in proximity of the support occurred. At a load level of $\alpha = 0.4$, unlike in the *C100* concrete deep beam, the previous relation was observed: the maximum deflection was at point x_{18} of the span at lower load levels, and the observed vertical displacements decreased monotonously towards the support. Also, at a load level of $\alpha = 0.5$, (Fig. 33) and unlike in the *C100* concrete deep beam, the previous relation was observed: no indications of concrete cracks were found in the central section at the lower load levels, unlike in the *C100* concrete deep beam. Whereas under a load of $\alpha = 0.6$, an unlimited increase was observed in the vertical displacements at the points adjacent to the span cross-section and indicative of the beam's carrying capacity depletion and imminent damage.

Fig. 8_3 shows the relation between the permanent vertical displacement in selected points in the deep beam's upper edge and the various loads $\alpha = P/P_0$. Up to a load of $\alpha = 0.5$, the maximum permanent deflection occurred in the span at point x_{306}, and the observed amplitudes of vertical displacements decreased monotonously towards the support. Under a load of $\alpha = 0.6$, an unlimited increase was observed in the vertical displacements near point x_{300}, indicative of the beam's carrying capacity depletion and imminent damage.

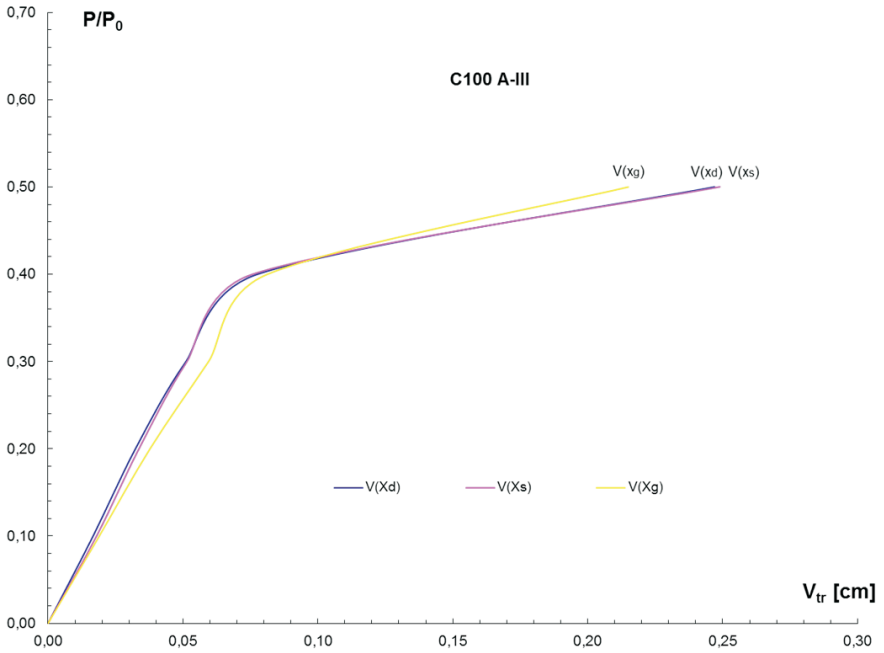

Fig. 7_1. Relation between the permanent dynamic displacement of the middle cross-section points and the load

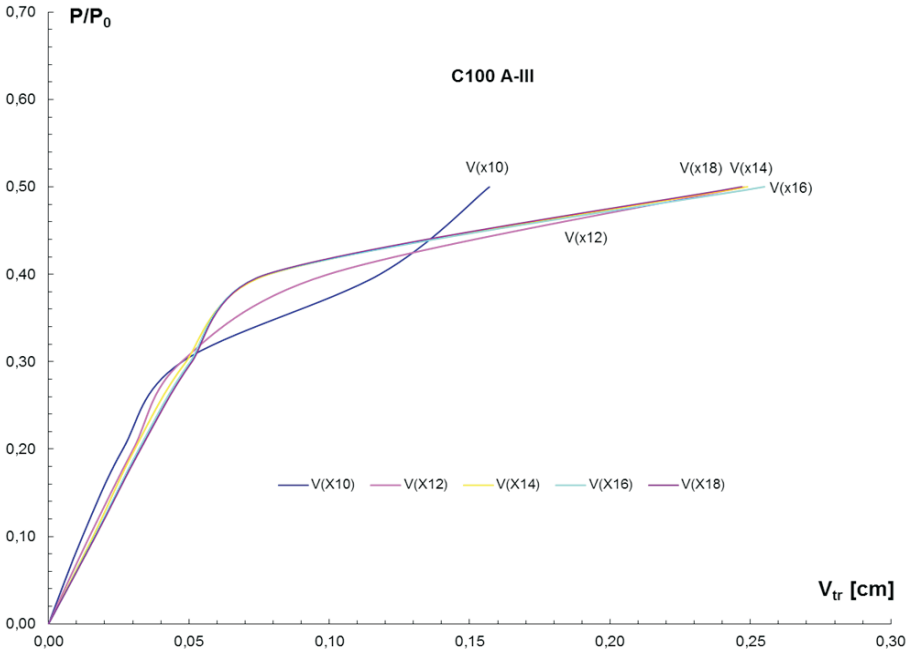

Fig. 7_2. Relation between the permanent dynamic displacement of the lower edge points and the load

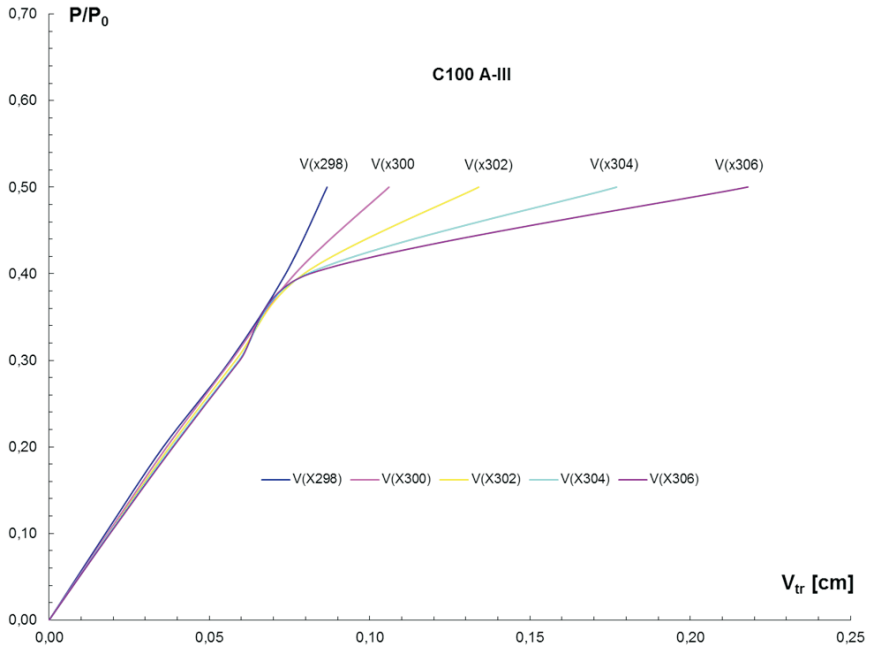

Fig. 7_3. Relation between the permanent dynamic displacement of the upper edge points and the load

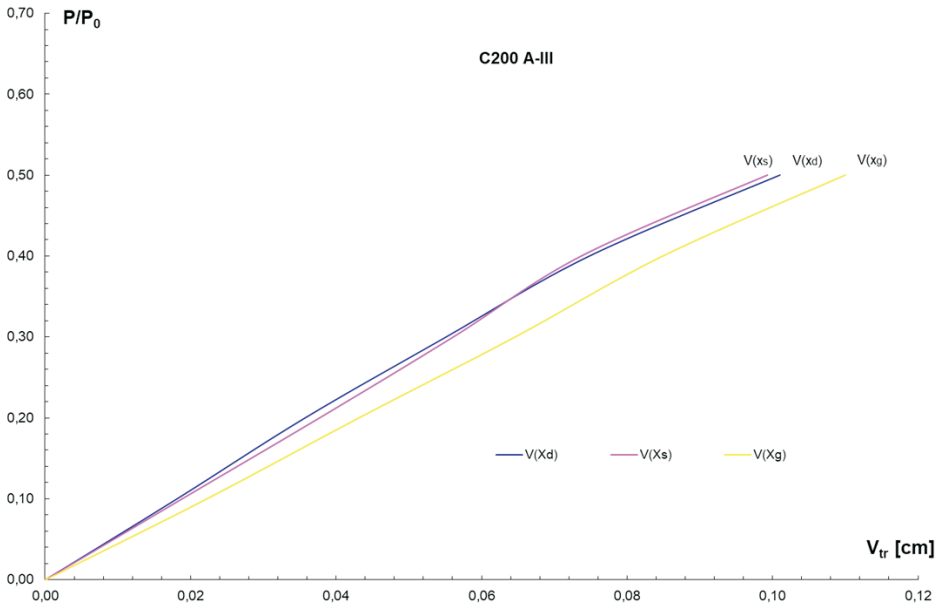

Fig. 8_1. Relation between the permanent dynamic displacement of the middle cross-section points and the load

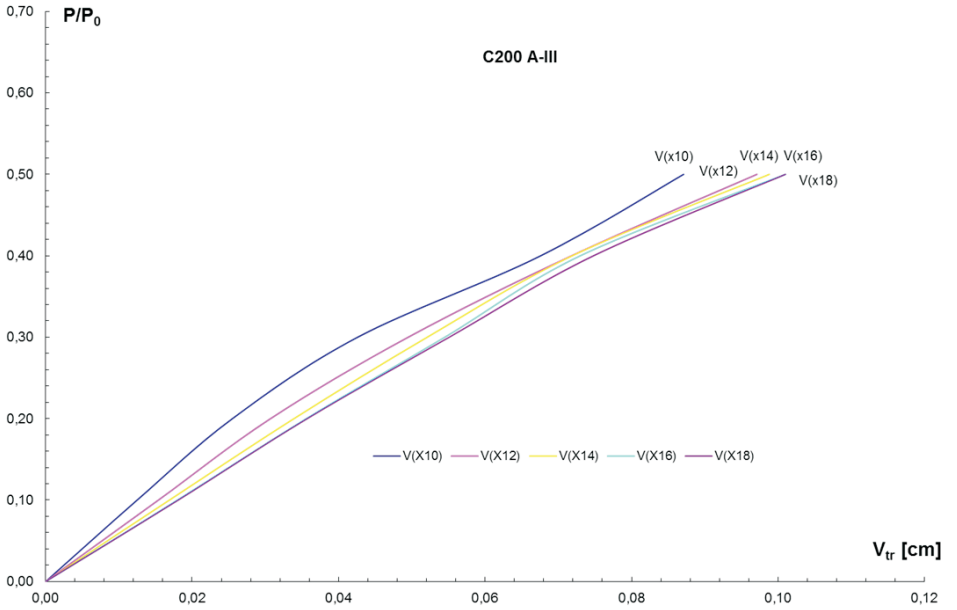

Fig. 8_2. Relation between the permanent dynamic displacement of the lower edge points and the load

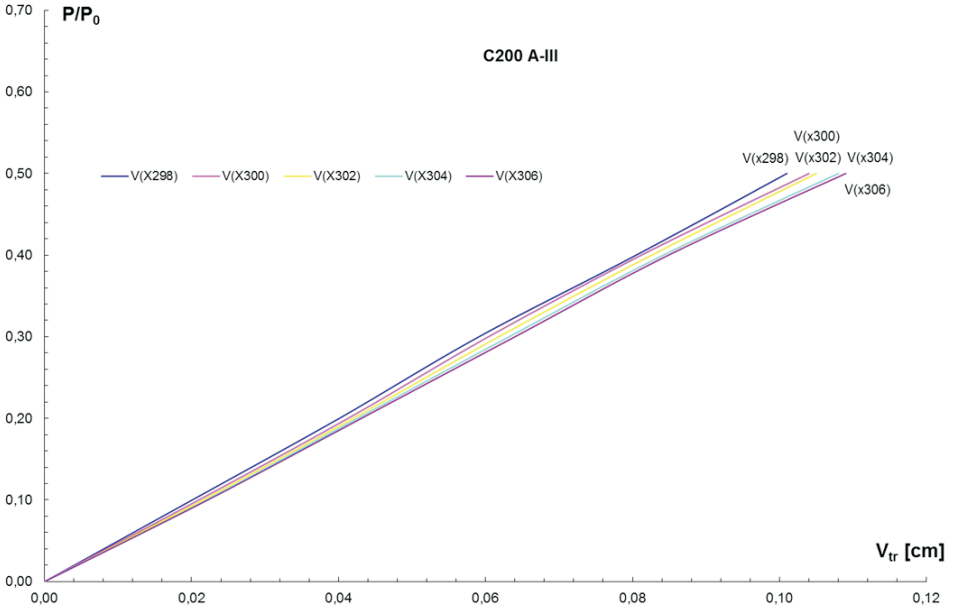

Fig. 8_3. Relation between the permanent dynamic displacement of the upper edge points and the load

Fig. 9 shows, for *C300* concrete and regular *A-III* steel reinforcement, the relation between the permanent dynamic displacements in selected points and the load.

Fig. 9_1 shows the variability of the permanent vertical displacements of the selected points in the middle cross-section under various loads $\alpha = P/P_0$. The results indicate, like for the *C100* and *C200* concrete beams, the known relationship between vertical displacements: $v(x_g) > v(x_s) > v(x_d)$. Under a load of $\alpha = 0.6$, (like in the *C100* and *C200* concrete beams) a lack of plastic process stabilisation can be observed, which ultimately led to the beam's lost load capacity.

Fig. 9_2 shows the variability of the permanent vertical displacement in selected points in the deep beam's lower edge under various loads $\alpha = P/P_0$. In the range of elastic capacity of the structure, the loads of $\alpha = 0.1$ and $\alpha = 0.2$ gave the maximum permanent deflection, just like in the *C100* concrete deep beam's span at point x_{18}, and the observed amplitude values of the vertical displacements decreased monotonously towards the support. The same behaviour of the structure was observed at a load level of $\alpha = 0.3$, when the cracking of the concrete in proximity of the support occurred. As the load was increased to $\alpha = 0.4$, propagation occurred of the partially cracked areas like in the *C200* concrete deep beam, i.e. in the shear zone only, but in the vertical upward direction only — which resulted in a decrease in the permanent vertical displacement in the points in the middle cross-section's vicinity, i.e. x_{16} and x_{18}. At a load level of $\alpha = 0.5$, like in the *C200* concrete deep beam, the previous relation was observed: the maximum permanent displacement was at point x_{18} of the span at lower load levels, and the observed vertical displacements decreased monotonously towards the support. At a load level of $\alpha = 0.5$, no concrete cracks were found in the middle cross-section, unlike in the *C100* concrete deep beam. Whereas at a load levelof $\alpha = 0.6$, further development of the scratched concrete area was visible. There was an unlimited increase of vertical displacements at the points adjacent to the span cross-section and indicative of the beam's carrying capacity depletion and imminent damage, just like in the C200 concrete deep beam.

Fig. 9_3 shows the variability of the permanent vertical displacement in selected points in the deep beam's lower edge under various loads $\alpha = P/P_0$. Like in the *C100* and *C200* beams, the maximum permanent displacement occurred in the span at point x_{306}, and the observed amplitude values of the vertical displacements decreased monotonously towards the support. At a load level of $\alpha = 0.6$, an unlimited increase of vertical displacements was observed in the middle cross-section's vicinity i.e. at points x_{306}, x_{304}, x_{302} and x_{300}, indicative of the beam's carrying capacity depletion and imminent damage.

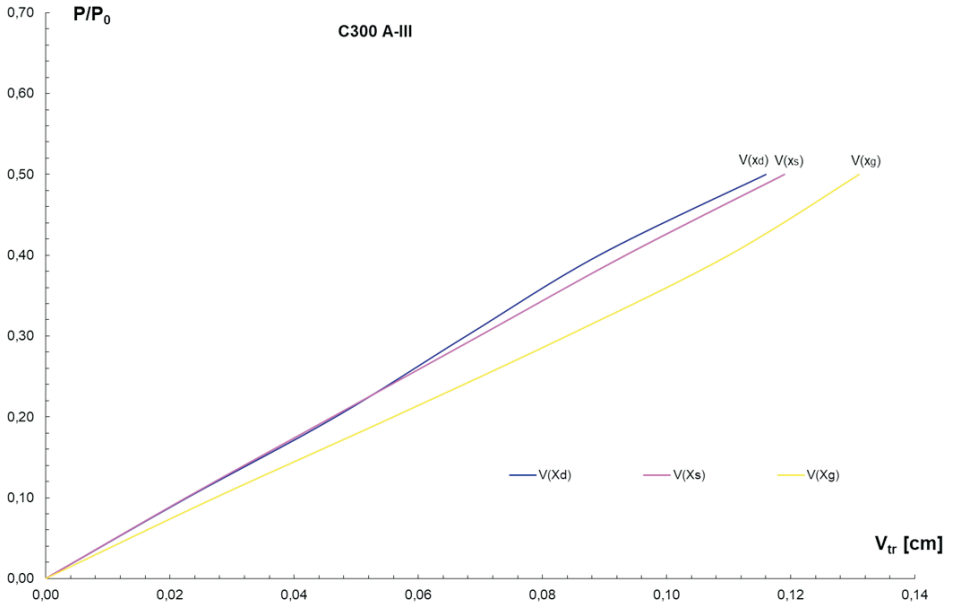

Fig. 9_1. Relation between the permanent dynamic displacement of the middle cross-section points and the load

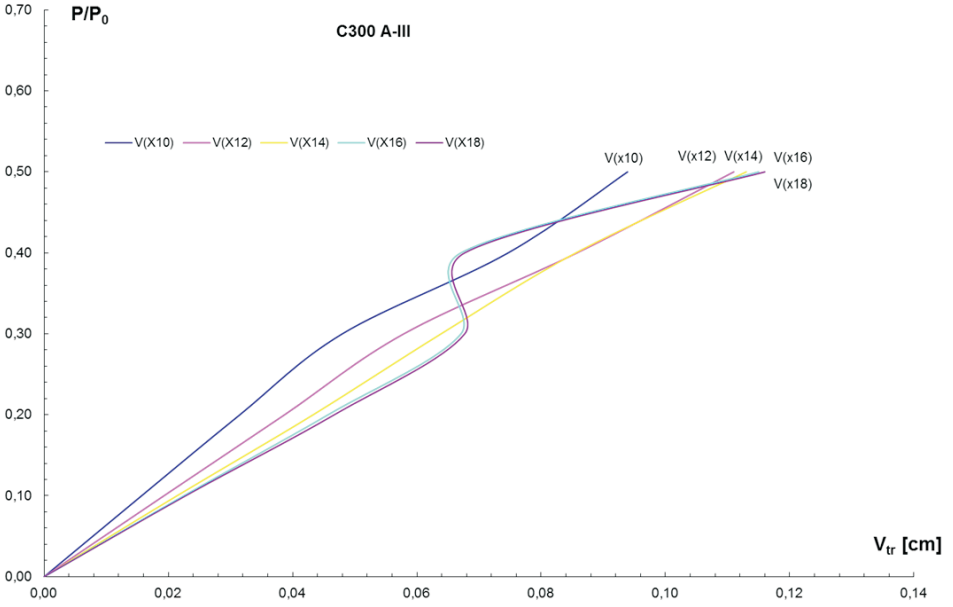

Fig. 9_2. Relation between the permanent dynamic displacement of the lower edge points and the load

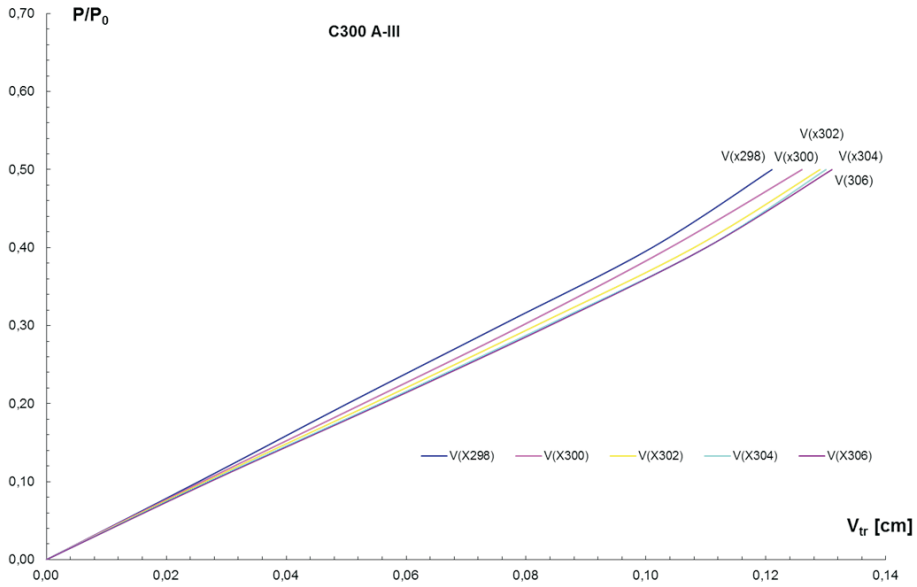

Fig. 9_3. Relation between the permanent dynamic displacement of the upper edge points and the load

Fig. 10 shows, for *C100* concrete and regular *A-H* steel reinforcement, the relation between the permanent dynamic displacements in selected points and the load.

Fig. 10_1 shows the variability of the permanent vertical displacements of the selected points in the middle cross-section under various loads $\alpha = P/P_0$. For a load level of $\alpha = 0.3$, in the elastic range and with a minor level of plastic processes in the concrete, the results indicate the relation known from the elastic solutions between vertical displacements: $v(x_g) > v(x_s) > v(x_d)$, like in the *A-III* steel reinforced *C100* concrete beam. As the load increases to the level of $\alpha = 0.4$, a significant increase of vertical displacements of the lower point x_d is observed. Despite scratching the concrete in the lower layers in the shear zone (like in the *A-III* steel reinforced beam), modification of the interrelations between the permanent vertical displacement of selected points in the middle cross-section did not occur, i.e. unlike in the *A-III* steel reinforced deep beam. With a further load increase to $\alpha = 0.5$, propagation of scratched areas in the shear zone occurred, however differently than in the A-*III* steel reinforced beam, i.e. only in the vertical direction. At the same time, no development of scratches in the span section was identified, unlike in the deep beam reinforced with A-*III* steel. This caused a modification of the interrelations between the vertical displacement of each point, different from the one in the *A-III* steel reinforced deep beam (for the same load): $v(x_g) > v(x_s) \cong v(x_g)$. At a load level of $\alpha = 0.6$, unlike in the *A-III* steel reinforced beam (for the same load), a further development of stable plastic processes was observed, which was manifested by stabilised vibration around permanent displacements of the observed points, and

a rapid increase in permanent vertical displacement of the bottom point x_d. Only at this level of loading (the same as in the deep beam reinforced with *A-III* steel at a load level of $\alpha = 0.5$) the propagation of scratched areas took place in the shear zone diagonally towards the centre of the span and there was a sudden propagation in the span area, which caused another modification of the interrelation between the change over time of each vertical displacement, different than in the deep beam reinforced with *A-III* steel at a load level of $\alpha = 0.5$): $v(x_s) > v(x_d) > v(x_g)$, which applies at intervals of reaching maximum amplitude of displacements. Unlike in the *A-III* steel reinforced bean, only at a load of $\alpha = 0.7$, the lack of plastic processes stabilisation can be observed as a result of the development of concrete crack zones in two areas: at first, diagonally from the support zone to the span section, and mainly in the middle cross-section, the beam's load capacity was lost.

Fig. 10_2 shows the variability of the permanent vertical displacement in the selected points in the deep beam's lower edge under various loads $\alpha = P/P_0$. In the range of elastic capacity of the structure, the loads $\alpha = 0.1$ and $\alpha = 0.2$ gave the maximum deflection, just like in the *A-III* steel reinforced deep beam, in the span at point x_{18}, and the observed amplitude values of the vertical displacements decreased monotonously towards the support. Also, at a load level of $\alpha = 0.3$, the same behaviour of the structure can be observed, when scratching of the concrete in the proximity of the support occurred. At a load level of $\alpha = 0.4$, just like in the A-III steel reinforced deep beam, a sudden increase in the permanent vertical displacement of point x_{10} occurs, exceeding the values of displacements of points adjacent to the central axis of the vertical symmetry. It is caused by the development of an area of scratched concrete in the proximity of that point — a propagation of the scratched area occurred in the vertical direction. Upon an additional increase of load to $\alpha = 0.5$, stabilisation of displacement of point x_{10} is observed. At the same time, an increase in displacements can be observed in the following vertical points: x_{12}, x_{14}, x_{16}, x_{18} close to the middle cross-section — this increase, however, is significantly smaller than in the case of the deep beam reinforced with *A-III* steel. It is caused by the difference in the development of concrete scratch areas. Currently, just as in the deep beam reinforced with *A-III* steel, a change occurred in the direction of propagation of the scratched area in the shear zone from vertical to diagonal towards the central section, however, unlike in the deep beam reinforced with *A-III* steel, concrete scratching in the lower layers of the central section did not occur. Only at a load level of $\alpha = 0.6$, a sudden increase was observed in vertical displacements, however, only from point x_{18} in the middle cross-section because of the manifestation of a new scratch area in middle cross-section (vertical scratch) and its sudden development in the vertical direction. At the same time, a further increase in the vertical displacements of point x_{10} is observed and a decrease in the permanent vertical displacements of points x_{12}, x_{14} and x_{16}, being a symptom of the beam's local load relief. The observed changes in the permanent displacements of the selected points indicate an evident change in the mechanism of the deep beam's cracks and stress/

strain caused by the change of reinforcing steel from *A-III* to *A-H*. For a load level of $\alpha = 0.7$, an unlimited increase in vertical displacements was observed successively at points x_{12}, x_{14}, x_{16} and x_{18}. It is an obvious sign of the depletion of carrying capacity and destruction of the analysed deep beam, however, at a different, higher load than in the deep beam reinforced with *A-III* steel.

Fig. 10_3 shows the variability of the permanent dynamic vertical displacement in selected points in the upper edge of the deep beam under various loads $\alpha = P/P_0$. Up to load $\alpha = 0.4$, the maximum permanent deflection, just like in the *A-III* steel reinforced deep beam, occurred in the span at point x_{306}, and the observed values of the vertical displacements decreased monotonously towards the support. The same behaviour of the structure can be observed at a load level of $\alpha = 0.5$, however, because of the advanced processes of concrete scratching, a differentiation of the permanent displacements of each point on the upper edge is visible. The same behaviour of the structure can be observed at a load level of $\alpha = 0.6$, however, at this load level, the deep beam reinforced with *A-III* steel was already damaged. At a load level of $\alpha = 0.7$, further development of the concrete scratch area is visible — an unimpeded increase in vertical displacements adjacent to the central section commences successively in points x_{304} and x_{306}, which signals depletion of carrying capacity and destruction of the analysed deep beam.

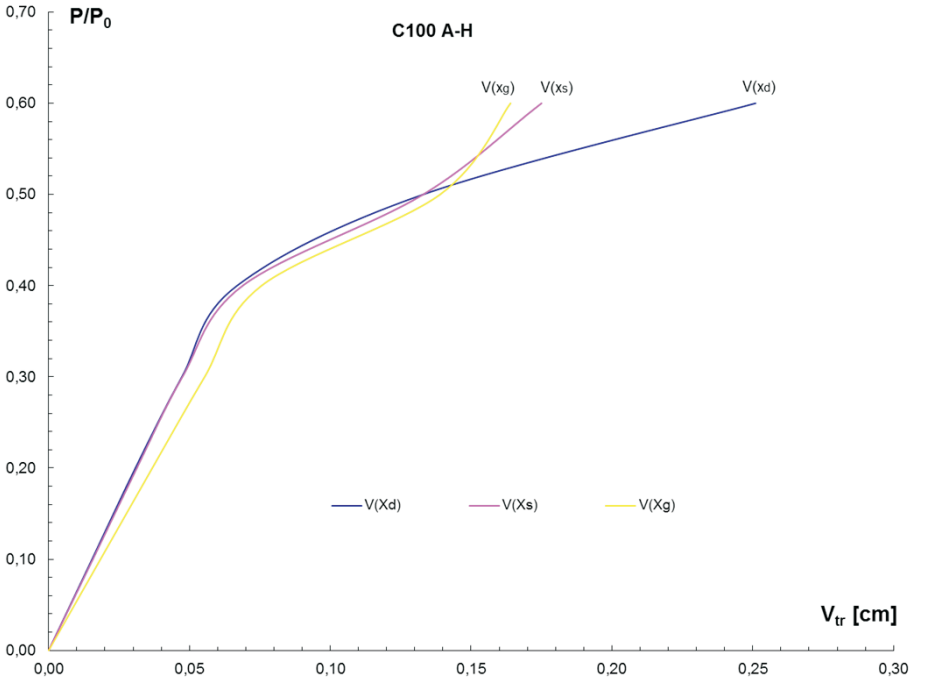

Fig. 10_1. Relation between the permanent dynamic displacement of the middle cross-section points and the load

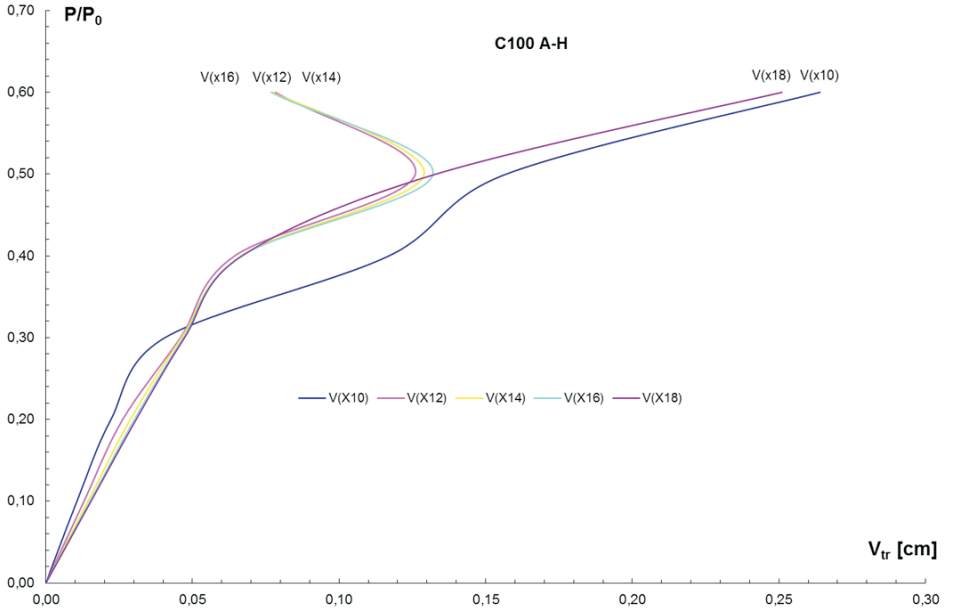

Fig. 10_2. Relation between the permanent dynamic displacement of the lower edge points and the load

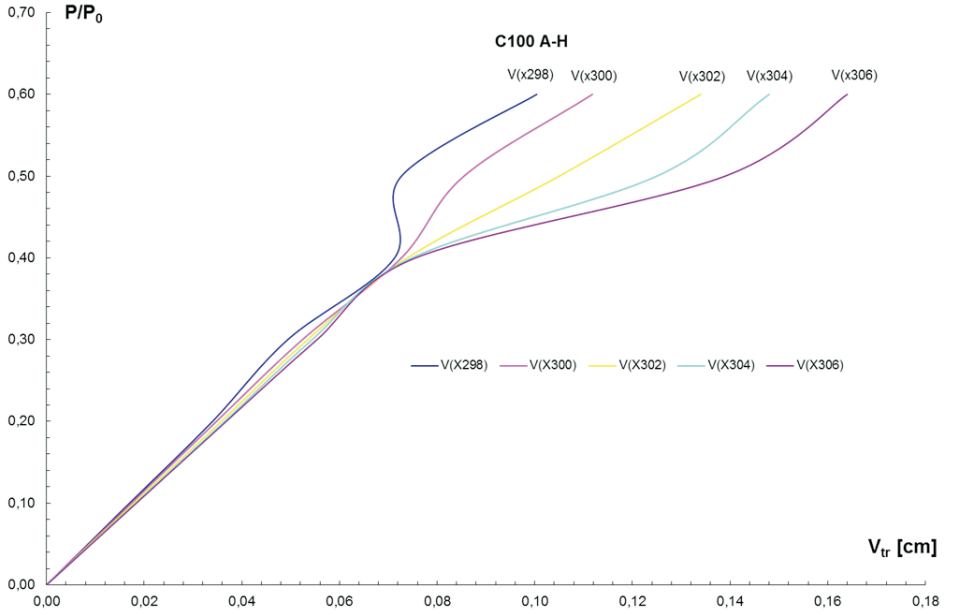

Fig. 10_3. Relation between the permanent dynamic displacement of the upper edge points and the load

Fig. 11 shows, for *C200* concrete and regular *A-H* steel reinforcement, the relation between the permanent dynamic displacements in selected points and the load.

Fig. 11_1 shows the variability of the permanent vertical displacements of selected points in the middle cross-section under various loads $\alpha = P/P_0$. Up to the a load level of $\alpha = 0.3$, like in the *A-III* steel reinforced concrete deep beam, the structure reacted in the elastic range at a low level of plastic processes in the concrete; the results indicated an analogical relation between the vertical displacements: $v(x_g) > v(x_s) > v(x_d)$. As the load increases to the level of $\alpha = 0.4$, an increase in the vertical displacements of the lower point x_d is observed. Because of cracks (scratching) of the concrete's lower layers in the shear zone, the interrelation was partially modified between changes in individual vertical displacements over time, like in the *A-III* steel reinforced deep beam: $v(x_g) > v(x_d) \cong v(x_s)$. As the load was increased to $\alpha = 0.5$, the propagation of the crack areas occurred analogically to that in the A-III steel reinforced concrete deep beam, i.e. in the shear zone only (in two directions: upwards and diagonally towards the span centre). As an effect of the development of the concrete cracking zones within a single area only, like in the deep beam reinforced with *A-III* steel, i.e. diagonally from the shear zone to the upper layers of the span cross-section, the beam's carrying capacity was lost at this load level already, unlike in the *A-III* steel reinforced deep beam. The maximum load level was changed by the replacement of reinforcing A-III grade steel with grade *A-H*.

Fig. 11_2 shows the variability of the permanent vertical displacement in the selected points in the deep beam's lower edge under various loads $\alpha = P/P_0$. In the range of elastic capacity of the structure, the loads of $\alpha = 0.1$ and $\alpha = 0.2$ gave the maximum deflection, just like in the *A-III* steel reinforced deep beam, in the span at point x_{18}, and the observed amplitude values of the vertical displacements decreased monotonously towards the support. The same behaviour of the structure was observed at a load level of $\alpha = 0.3$, when the cracking of the concrete in proximity of the support occurred. At a load level of $\alpha = 0.4$, like in the *A-III* steel reinforced deep beam, the previous relation was observed: the maximum permanent deflection was at point x_{18} of the span at lower load levels, and the observed vertical displacements decreased monotonously towards the support. Whereas at a load of $\alpha = 0.5$, an unlimited increase was observed in the vertical displacements at the points adjacent to the span cross-section and indicative of the beam's carrying capacity depletion and imminent damage.

Fig. 11_3 shows the variability of the permanent dynamic vertical displacement in the selected points in the upper edge of the deep beam under various loads $\alpha = P/P_0$. At the loads of $\alpha = 0.1$, $\alpha = 0.2$, $\alpha = 0.3$ and $\alpha = 0.4$, the maximum permanent deflection, just like in the *A-III* steel reinforced deep beam, occurred in the span at point x_{306}, and the observed values of the vertical displacements decreased monotonously towards the support. At a load of $\alpha = 0.5$, further development of the concrete cracking area was found. There was an unlimited increase in vertical displacements near point x_{300}, indicative of the beam's carrying capacity depletion and imminent damage, just as in the deep beam reinforced with *A-III* steel at a load level of $\alpha = 0.6$.

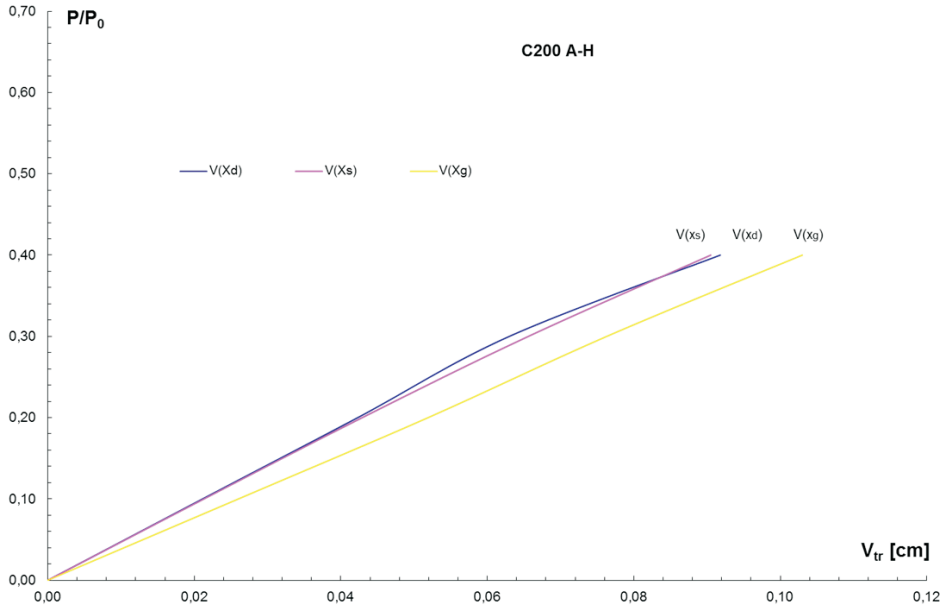

Fig. 11_1. Relation between the permanent dynamic displacement of the middle cross-section points and the load

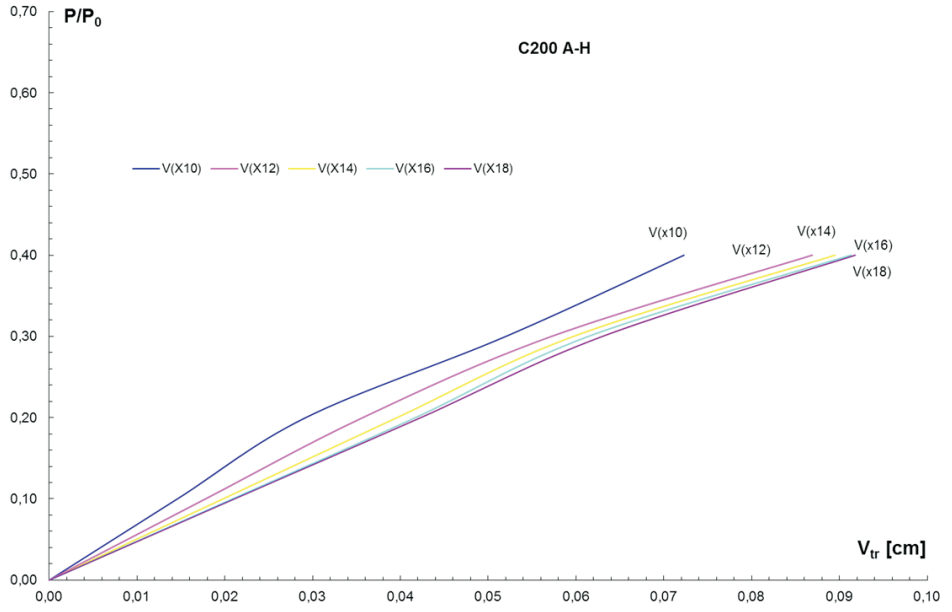

Fig. 11_2. Relation between the permanent dynamic displacement of the lower edge points and the load

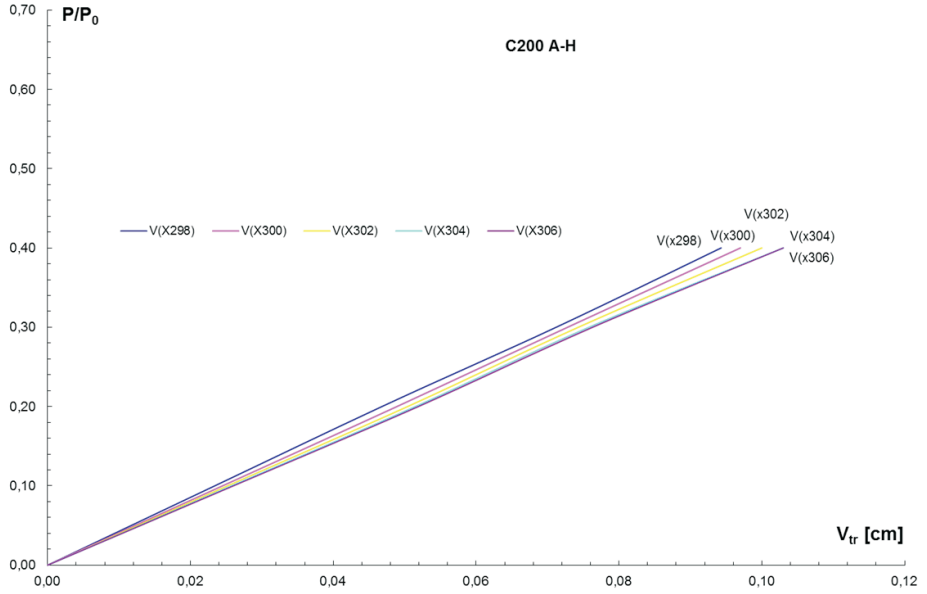

Fig. 11_3. Relation between the permanent dynamic displacement of the upper edge points and the load

Fig. 12 shows, for *C300* concrete and regular *A-H* steel reinforcement, the relation between the permanent dynamic displacements in the selected points and the load.

Fig. 12_1 shows the variability of the permanent vertical displacements of the selected points in the middle cross-section under various loads $\alpha = P/P_0$. Up to a load level of $\alpha = 0.3$, like in the *A-III* steel reinforced concrete deep beam, the structure reacted in the elastic range at a low level of plastic processes in the concrete; the results indicated an analogical relation between the vertical displacements: $v(x_g) > v(x_s) > v(x_d)$. As the load was increased to $\alpha = 0.4$, the permanent vertical displacements of the lower point x_d increased just like in the deep beams reinforced with *A-III* steel. Because of the cracks (scratching) of the concrete in the lower layers of the shear zone, there was a partial modification of the interrelation of the changes of individual vertical displacements over time: $v(x_g) > v(x_d) \cong v(x_s)$. As the load was further increased to $\alpha = 0.5$, propagation of the crack areas occurred only in part of the crack area extent found in the A-III steel reinforced deep beam, in that the propagation was observed in the upward vertical direction in the shear zone only. The effect of this was not unlike in the *A-III* steel reinforced deep beam: it did not modify the interrelation of the changes of individual vertical displacements over time, i.e. $v(x_g) > v(x_d) \cong v(x_s)$. At a load level of $\alpha = 0.6$, like in the *A-III* steel reinforced deep beam, a lack of stabilisation of plastic processes was observed and manifested with a stabilised vibration around the observed points' permanent displacements under lower loads. However, the process of vibrating motion stability loss was more violent than in the deep beam reinforced with A-III steel.

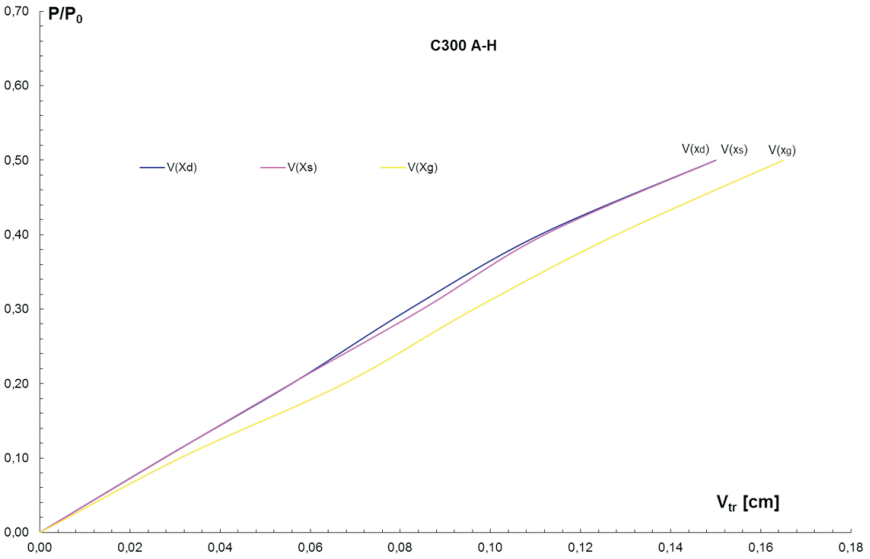

Fig. 12_1. Relation between the permanent dynamic displacement of the middle cross-section points and the load

Fig. 12_2 shows the variability of the permanent vertical displacement in the selected points in the deep beam's lower edge under various loads $\alpha = P/P_0$. In the range of elastic capacity of the structure, the loads of $\alpha = 0.1$ and $\alpha = 0.2$ gave the maximum deflection, just like in the *A-III* steel reinforced deep beam, in the span at point x_{18}, and the observed amplitude values of the vertical displacements decreased monotonously towards the support. The same behaviour of the structure was observed at a load level of $\alpha = 0.3$, when cracking of the concrete in proximity of the support occurred. At the load levels of $\alpha = 0.4$ and $\alpha = 0.5$, like in the *A-III* steel reinforced deep beam, the previous relation was observed: the maximum permanent deflection was at point x_{18} of the span at lower load levels, and the observed vertical displacements decreased monotonously towards the support. At the same time, at a load level of $\alpha = 0.5$, no concrete cracks were found in the middle cross-section, unlike in the *A-III* steel reinforced deep beam. Whereas at a load level of $\alpha = 0.6$, an unlimited increase was observed in the vertical displacements near the span cross-section, indicative of the beam's carrying capacity depletion and imminent damage, just like in the deep beam reinforced with *A-III* steel.

Fig. 12_3 shows the variability of the permanent dynamic vertical displacement in the selected points in the upper edge of the deep beam under various loads $\alpha = P/P_0$. At a load increase to $\alpha = 0.4$, the maximum permanent deflection, just like in the *A-III* steel reinforced deep beam, occurred in the span at point x_{306}, and the observed values of the vertical displacements decreased monotonously towards the support. The same behaviour of the structure, like in the *A-III* steel reinforced deep beam, was observed at a load level of $\alpha = 0.5$, i.e. there was no evidence of dynamic balance differentiation, no permanent displacement of the points on the upper

edge occurred. Under a load of $\alpha = 0.6$, an unlimited increase was observed in the vertical displacements near point x_{298}, indicative of the beam's carrying capacity limit with a failure of the deep beam. There were no significant differences in the response of the *C300* concrete deep beam between its different reinforcement steel grades, i.e. upon replacement of regular *A-III* grade steel with *A-H*.

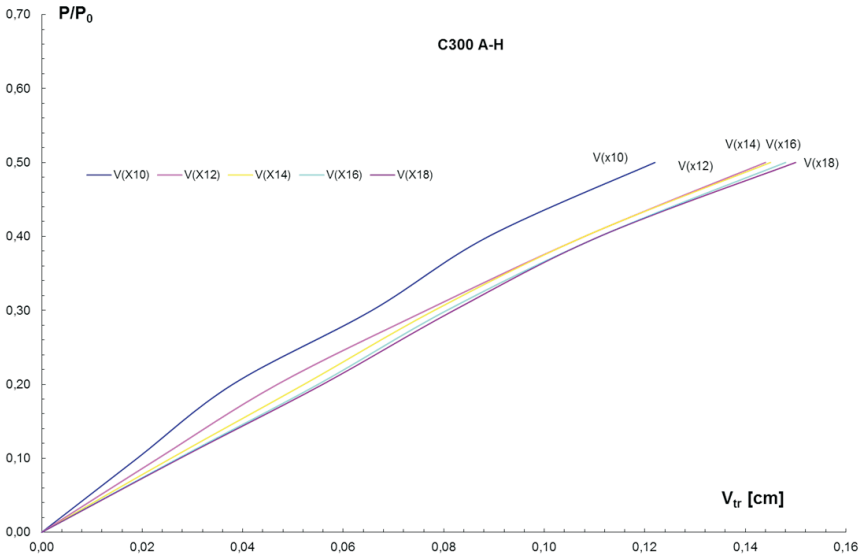

Fig. 12_2. Relation between the permanent dynamic displacement of the lower edge points and the load

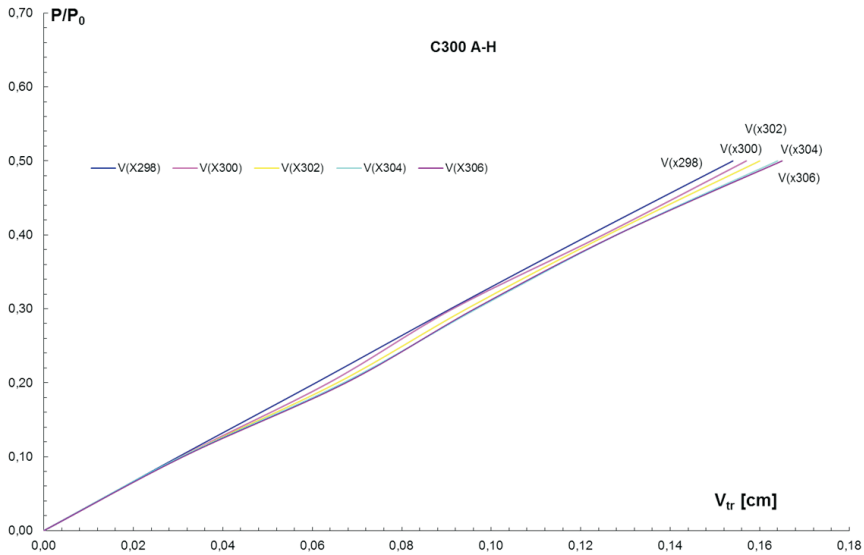

Fig. 12_3. Relation between the permanent dynamic displacement of the upper edge points and the load

3. Conclusion

The paper estimates the dynamic load carrying capacity of a rectangular steel--reinforced concrete deep beam made of very high strength *C100, C200* or *C300* grade concrete and reinforced with regular *A-III* or high-strength *A-H* steel. The dynamic load carrying capacity was estimated based on the observation of changes in the vertical displacements of selected points on the beam's lower and upper edges and in the middle cross-section. By analysis, it was established that increasing the strength of either the concrete or steel can affect both the reinforced concrete beam's dynamic load carrying capacity, and the stress/strain and damage mechanisms in the form of a differentiated process of concentration and changes of concrete matrix crack areas. The presented results confirmed it is necessary to investigate the effect of the constitutive model parameters of the very high-strength concrete and the increased--strength steel on the effort mechanism of reinforced concrete elements. A complete analysis of the impact of the analysed factors will allow the desirability of designing such elements using a very high strength concrete as well as high strength steel to be assessed. The results presented in this paper confirmed the correctness of the assumptions and deformation models of concrete and steel as well as the effectiveness of the methods of analysis proposed for the problems of numerical simulation of the dynamic behaviour of reinforced concrete deep beams under dynamic loads.

The study was carried out as a result of research tasks carried out within the framework of statutory research no 934, carried out in the Faculty of Civil Engineering and Land Surveying of the Military University of Technology.

Received February 26, 2018. Revised July 3, 2018.

Paper translated into English and verified by company SKRIVANEK sp. z o.o., 22 Solec Street, 00-410 Warsaw, Poland.

REFERENCES

[1] Cichorski W., Stolarski A., *Modelling of inelastic behaviour of reinforced concrete deep beam*, Journal of Achievements in Materials and Manufacturing Engineering, 44, 1, 2016, 37-44.

[2] Cichorski W., Stolarski A., *Analizy stanu przemieszczenia niesprężystej tarczy żelbetowej obciążonej statycznie*, Biuletyn WAT, 50, 5, 2001, 5-20.

[3] Cichorski W., Stolarski A., *Analizy wytężenia tarczy żelbetowej z materiałów konstrukcyjnych bardzo wysokich wytrzymałości*, Biuletyn WAT, 65, 4, 2016, 143-165.

[4] Kamińska M.E., Miszczak J., *Experimental and analytical aspects of HSC confinement in tied slender columns*, 3rd International Conference on Analytical Models and New Concepts in Mechanics of Concrete Structures, Wrocław – Świeradów Zdrój, Poland, June 16-19, 1999, 109-114.

[5] Kleiber M., *Metoda elementów skończonych w nieliniowej mechanice kontinuum*, PWN, Warszawa, 1985.

[6] Leonhardt F., Walther R., *Wandartige träger*, Report, Deutscher Asschüb für Stahlbeton, 229, Germany, Berlin, 1966.

[7] Lewiński P.M., *Nieliniowa analiza płyt i tarcz żelbetowych metodą elementów skończonych*, PWN, Warszawa–Łódź, 1990.

[8] Majorama C.E., Salomoni V.A., Schrefler B.A., *A constitutive relationship for high performance and ultra high performance concrete*, The Euro-C 1998 Conference on Computational Modelling of Concrete Structures, Badgastein, Austria, 31 March–3 April 1998, 1, 203-208.

[9] Marzec I., Tejchman J., Winnicki A., *Computational simulations of concrete behaviour under dynamic conditions using elasto-visco-plastic model with non-local softening*, Computers & Concrete, 15, 4, 2015, 515-545.

[10] Miedziałowski Cz., *The static and dynamic analysis of building structures. Selected problems.*, Oficyna Wydawnicza Politechniki Białostockiej, Białystok, 2015.

[11] Ožbolt J., Meštrović D., Li Y.J., Eligausen R., *Compression Failure of Beams Made of Different Concrete Types and Sizes*, Journal of Structural Engineering, 126, 2, 2000, 200-209.

[12] Rashid M.A., Mansur M.A., *Reinforced high-strength concrete beams in flexure*, ACI „Structural Journal", vol. 102, no. 3, 2005, 462-471.

[13] Stolarski A., *Dynamic strength criterion for concrete*, Journal of Engineering Mechanics, ASCE, vol. 130, 12, 2004, 1428-1435.

[14] Stolarski A., *Model dynamicznego odkształcania betonu*, Archiwum Inżynierii Lądowej, 37, 3-4, 1991, 405-447.

[15] Stolarski A., Cichorski W., *Modelowanie statycznego i dynamicznego zachowania tarcz żelbetowych*, Komitet Inżynierii Lądowej i Wodnej PAN, Studia z Zakresu Inżynierii, 51, Warszawa, 2002.

[16] Stolarski A., Cichorski W., *Influence of high strength of concrete and reinforced steel on dynamic behavior of reinforced concrete deep beams*, Proceedings of the 12rd International Conference on Shock & Impact Loads on Structures, Singapore, 15-16 June 2017, 159-168.

[17] Stolarski A., Cichorski W., *Oszacowanie nośności tarczy żelbetowej z uwzględnieniem betonu bardzo wysokiej wytrzymałości*, Biuletyn WAT, 51, 2, 2002, 49-67.

[18] Winnicki A., Pearce C.J. and Bićanić N., *Viscoplastic Hoffman consistency model for concrete*, Comput. & Struct., 79, 2001, 7-19.

W. CICHORSKI

Oszacowanie dynamicznej nośności tarczy żelbetowej z materiałów konstrukcyjnych o bardzo wysokiej wytrzymałości

Streszczenie. W pracy przedstawiono analizę dynamicznej nośności prostokątnych tarcz żelbetowych wykonanych z materiałów o bardzo wysokiej wytrzymałości obciążonych dynamicznie z uwzględnieniem fizycznych nieliniowości materiałów konstrukcyjnych: betonu i stali zbrojeniowej. Rozwiązanie otrzymano na podstawie metody zaprezentowanej w pracy [15]. Wyznaczono dynamiczną nośność tarczy żelbetowej. Przedstawiono wyniki rozwiązań numerycznych ze szczególnym uwzględnieniem wpływu bardzo wysokiej wytrzymałości betonu i stali na dynamiczną nośność tarczy żelbetowej. Wykazano poprawność przyjętych założeń i modeli odkształcenia betonu i stali oraz efektywność metody analizy proponowanej w pracy [1, 15] dla problemów numerycznej symulacji zachowania tarcz żelbetowych.

Słowa kluczowe: mechanika konstrukcji, konstrukcje żelbetowe, tarcze, obciążenie dynamiczne, nieliniowość fizyczna

DOI: 10.5604/01.3001.0012.8483